Amino Acids (2015) 47:1409–1419
DOI 10.1007/s00726-015-1975-4

ORIGINAL ARTICLE

PET imaging of insulin-like growth factor type 1 receptor expression with a ^{64}Cu-labeled Affibody molecule

Xinhui Su[1,2] · Kai Cheng[2] · Yang Liu[2] · Xiang Hu[2] · Shuxian Meng[2] · Zhen Cheng[2]

Received: 3 March 2015 / Accepted: 29 March 2015 / Published online: 9 April 2015

Abstract The insulin-like growth factor 1 receptor (IGF-1R) serves as an attractive target for cancer molecular imaging and therapy. Previous single photon emission computerized tomography (SPECT) studies showed that the IGF-1R-targeting Affibody molecules ^{99m}Tc-$Z_{IGF1R:4551}$-GGGC, $[^{99m}Tc(CO)_3]^+$-$(HE)_3$-$Z_{IGF1R:4551}$ and ^{111}In-DOTA-$Z_{IGF1R:4551}$ can discriminate between high and low IGF-1R-expression tumors and have the potential for patient selection for IGF-1R-targeted therapy. Compared with SPECT, positron emission tomography (PET) may improve imaging of IGF-1R-expression, because of its high sensitivity, high spatial resolution, strong quantification ability. The aim of the present study was to develop the ^{64}Cu-labeled NOTA-conjugated Affibody molecule $Z_{IGF-1R:4:40}$ as a PET probe for imaging of IGF-1R-positive tumor. An Affibody analogue (Ac-Cys-$Z_{IGF-1R:4:40}$) binding to IGF-1R was site-specifically conjugated with NOTA and labeled with ^{64}Cu. Binding affinity and specificity of ^{64}Cu-NOTA-$Z_{IGF-1R:4:40}$ to IGF-1R were evaluated using human glioblastoma U87MG cells. Small-animal PET, biodistribution, and metabolic stability studies were conducted on mice bearing U87MG xenografts after the injection of ^{64}Cu-NOTA-$Z_{IGF-1R:4:40}$ with or without co-injection of unlabeled Affibody proteins. The radiosynthesis of ^{64}Cu-NOTA-$Z_{IGF-1R:4:40}$ was completed successfully within 60 min with a decay-corrected yield of 75 %. ^{64}Cu-NOTA-$Z_{IGF-1R:4:40}$ bound to IGF-1R with low nanomolar affinity (K_D = 28.55 ± 3.95 nM) in U87MG cells. ^{64}Cu-NOTA-$Z_{IGF-1R:4:40}$ also displayed excellent in vitro and in vivo stability. In vivo biodistribution and PET studies demonstrated targeting of U87MG gliomas xenografts was IGF-1R specific. The tumor uptake was 5.08 ± 1.07 %ID/g, and the tumor to muscle ratio was 11.89 ± 2.16 at 24 h after injection. Small animal PET imaging studies revealed that ^{64}Cu-NOTA-$Z_{IGF-1R:4:40}$ could clearly identify U87MG tumors with good contrast at 1–24 h after injection. This study demonstrates that ^{64}Cu-NOTA-$Z_{IGF-1R:4:40}$ is a promising PET probe for imaging IGF-1R positive tumor.

Keywords Affibody · IGF-1R · PET · ^{64}Cu · NOTA

Introduction

The insulin-like growth factor receptor (IGF-1R), a member of the family of transmembrane protein tyrosine kinases, is a well-established tumor biomarker that is overexpressed in a wide variety of cancers, including breast, prostate, lung, colorectal, gastric cancer, and glioma (Arcaro 2013; Singh et al. 2014). Increased IGR-1R signaling has shown to lead to activation of distinct signaling pathways, including the phosphatidylinositol 3-kinase (PI3 K)-Akt pathway and the Ras/Raf/mitogen-activated protein (MAP) kinase pathway, resulting in increased tumor cell differentiation, proliferation, and migration (Xue et al. 2012). Mounting evidence has demonstrated that there is a correlation between IGF-1R overexpression and tumor metastasis formation, therapy resistance, poor prognosis, and short survival (Pollak 2008). Therefore, IGF-1R has great value as a molecular

Handling Editor: G. Lubec.

✉ Zhen Cheng
zcheng@stanford.edu

[1] Department of Nuclear Medicine, Zhongshan Hospital Xiamen University, Xiamen, China

[2] Molecular Imaging Program at Stanford (MIPS), Department of Radiology, Bio-X Program and Stanford Cancer Center, Stanford University School of Medicine, Stanford, CA 94305, USA

target for therapeutic intervention, a prognostic indicator of patient survival, and a predictive marker of the response to antineoplastic therapy. Accordingly, IGF-1R inhibition using monoclonal antibodies and small-molecule tyrosine kinase inhibitors is considered as a promising strategy for cancer therapy (Pollak 2012; Haisa 2013). Both preclinical and clinical data suggest that accurate assessment of IGF-1R expression is essential for stratifying patients for anti-IGF-1R therapy (Zha et al. 2009; Gong et al. 2009; Ozkan 2011).

Nowadays, IGF-1R expression is determined on tumor biopsies using histologic immuno-histochemistry. However, this method is associated with invasive acquisition of multiple biopsies from a patient. In addition, the accuracy of biopsy-based methods is limited: samplings may be non-representative because of intratumoral expression heterogeneity, and molecular target level may be discordant in primary tumors and metastases (Tolmachev et al. 2012). Therefore, in vivo imaging of IGF-1R expression offers a more accurate and real-time assay of IGF-1R expression both for patient stratification and monitoring expression-level changes in response to therapy (Tolmachev et al. 2010), without such biopsy-associated pitfalls and the need of repetitive invasive biopsies.

A variety of small molecules and monoclonal antibodies based upon IGF-1R have been labeled with radionuclide ^{111}In for single photon emission computed tomography (SPECT) molecular imaging of IGR-1R expression (Cornelissen et al. 2008; Fleuren et al. 2011; Heskamp et al. 2012). But, for the small molecules, the probes generally show rapid blood clearance, very low tumor uptake; thus, the imaging quality is poor; for antibody or antibody fragments, their large size results in slow tumor accumulation and slow clearance from the circulation. These drawbacks severely hamper their clinical applications. Recently, one novel class of promising platform for developing imaging or therapeutic agents for different molecular targets is Affibody molecules. Affibody molecules are based on a 58 amino acid residue protein domain, derived from one of the IgG-binding domains of staphylococcal protein A, and have been engineered to be chemically stable and to bind target proteins with high affinity (Friedman et al. 2007; Cheng et al. 2010). In our previous study, Affibody molecules $Z_{HER2:477}$ and $Z_{EGFR:1907}$ labeled with ^{18}F or ^{64}Cu have shown rapid human epidermal growth factor receptor 2 (HER2) or epidermal growth factor receptor (EGFR) positive tumor targeting ability and high imaging contrast within a short period (for example, 0.5–1 h) after injection (Miao et al. 2010; Ren et al. 2012; Miao et al. 2012; Su et al. 2014). These results have encouraged us to further develop this type of Affibody molecules for positron emission tomography (PET) imaging of many other important tumor biomarkers including IGF-1R.

Some anti-IGF-1R Affibody molecules have been reported recently (Li et al. 2010). Among them, Affibody molecule $Z_{IGF1R:4551,}$ an affinity-matured variant of $Z_{4:40}$ with a C-terminal cysteine, was radiolabeled with ^{111}In (Tolmachev et al. 2012) or ^{99m}Tc (Orlova et al. 2013; Mitran et al. 2015) and evaluated using IGF-1R expression DU-145 or MCF-7 tumor xenografts. SPECT imaging and biodistribution studies demonstrated that these probes based on $Z_{IGF1R:4551}$ displayed specific and good tumor accumulation. However, imaging of IGF-1R expression with Affibody molecule can be improved by the use of positron-emitting radionuclides such as ^{64}Cu, because of the higher sensitivity and better quantification of positron emission tomography (PET) than SPECT. Lately, a new method was described for labeling of NOTA-conjugated peptides with ^{64}Cu, which is based on the formation of $^{64}CuCl_2$ and its complexation by NOTA (Ait-Mohand et al. 2011; Prasanphanich et al. 2007). This method allows rapid and efficient labeling of peptides and proteins with ^{64}Cu than DOTA (Zhang et al. 2011). In this study, we aimed to develop an IGF-1R Affibody molecule based PET probe for the imaging of an IGF-1R positive tumor. A $Z_{4:40}$ analogue, Ac-Cys-$Z_{IGF-1R:4:40}$, was first synthesized so that the protein can be site-specifically conjugated with maleimide monoamide NOTA (MMA-NOTA) through the C-terminal cysteine. The resulting bioconjugate, NOTA-$Z_{IGF-1R:4:40,}$ was then radiolabeled with ^{64}Cu (Fig. 1). The in vitro and in vivo biologic profiles of ^{64}Cu-NOTA-$Z_{IGF-1R:4:40}$ were evaluated in cultured U87MG cells with high IGF-1R expression levels and nude mice bearing subcutaneous U87MG tumors. Finally, the ability of ^{64}Cu-NOTA-$Z_{IGF-1R:4:40}$ to image IGF-1R expression in living mice was evaluated with small-animal PET.

Materials and methods

Materials

MMA-NOTA was purchased from CheMatech Inc. (Dijon, France). Phosphate-buffered saline (PBS), Eagle's Minimum Essential Medium (EMEM), 10 % fetal bovine serum (FBS), 1 % penicillin–streptomycin, 0.1 % trypsin, trypsin–EDTA and TrypLE-Express were purchased from Invitrogen Life Technologies (Carlsbad, California). Dimethylsulfoxide (DMSO) and acetonitrile (MeCN) were purchased from Fisher Scientific (Pittsburgh, PA, USA). Dichloromethane (DCM), triethylamine, *N*-hydroxybenzotriazole-hydrate (HOBT), ethyl acetate, trifluoroacetic acid (TFA), thioanisole (TIS), ethanedithiol (EDT), ethylene-diamine-tetra-acetic acid (EDTA), dithiothriotol (DTT), dimethylformamide (DMF), mouse serum, and all other standard synthesis reagents were purchased from Sigma-Aldrich

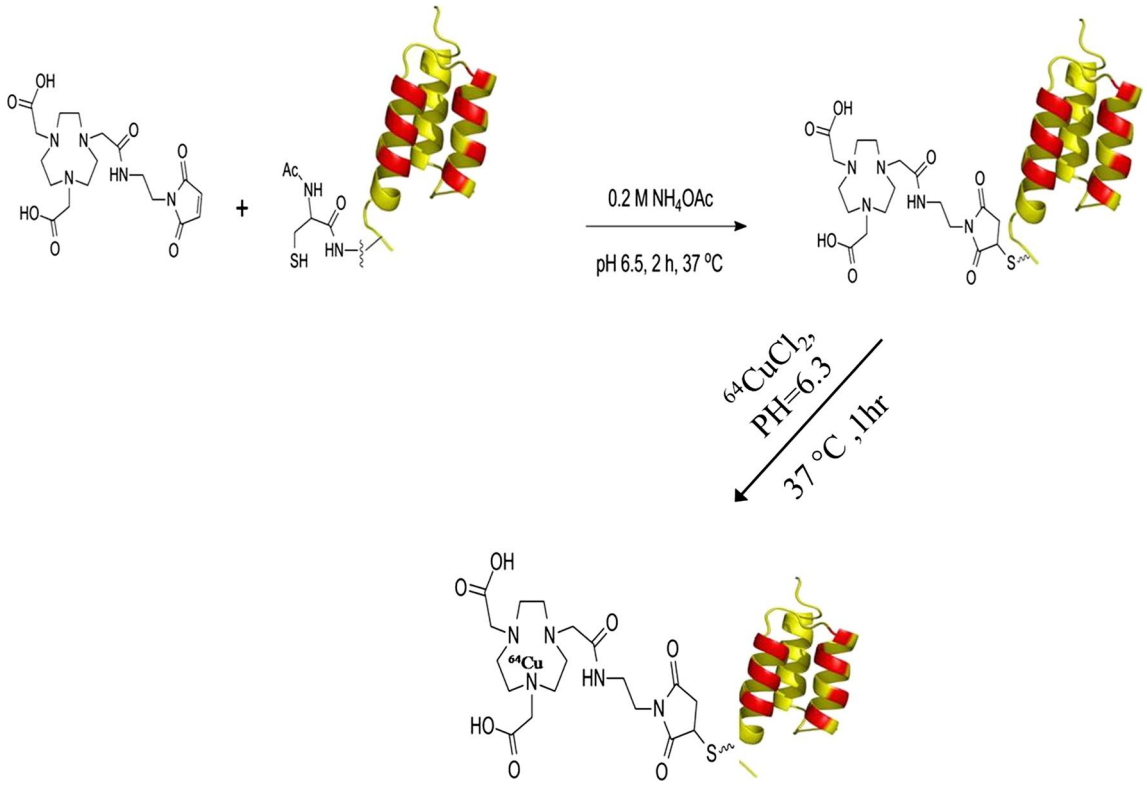

Fig. 1 Scheme of radiosynthesis of ^{64}Cu-NOTA-$Z_{IGF\text{-}1R:4:40}$

Chemical Co. (St. Louis, MO, USA). All chemicals were used without further purification. Human glioblastoma cell line U87MG was obtained from the American Type Tissue Culture Collection (Manassas, VA, USA). Female nude mice were purchased from Charles River Laboratories (Boston, MA, England). The radionuclide, ^{64}Cu, was provided by the Department of Medical Physics, University of Wisconsin at Madison.

Production of the Ac-Cys-$Z_{IGF\text{-}1R:4:40}$ Affibody molecule

The Affibody molecule Ac-Cys-$Z_{IGF\text{-}1R:4:40}$ (Ac-CVDNK-FNKEGFYAAIEIL-ALPNLNRKQSTAFISSLEDDP-SQSANLLAEAKKLNDAQAPK-NH2) (Li et al. 2010) was synthesized on a CS Bio CS336 instrument (CS Bio Company, Menlo Park, CA, USA) in our laboratory according to a method described earlier (Miao et al. 2010). Purified peptide was dissolved in water, and concentration was determined by amino acid analysis (Molecular Structure Facility, University of California, Davis, CA, USA). Peptide purity and molecular mass were determined by analytic scale reversed-phase high-performance liquid chromatography (RP-HPLC, model: 3000 HPLC System, Dionex Corporation, Sunnyvale, CA, USA) and matrix-assisted laser desorption/ionization–time of flight mass spectrometry (MALDI-TOF–MS, model: Perseptive Voyager-DE RP Biospectrometer, Framinghan, Massachusetts), or electrospray ionization mass spectrometry (ESI–MS, model: Micromass ZQ single quadrupole LC–MS, Milford, Massachusetts) as previously described (Miao et al. 2010).

Radiosynthesis of ^{64}Cu-NOTA-$Z_{IGF\text{-}1R:4:40}$

The Affibody molecule Ac-Cys-$Z_{IGF\text{-}1R:4:40}$ was conjugated with NOTA and radiolabeled with ^{64}Cu similarly to the coupling of MMA-DOTA described earlier (Fig. 1) (Miao et al. 2010). First, Affibody molecules Ac-Cys-$Z_{IGF\text{-}1R:4:40}$ were conjugated with the bifunctional chelator MMA-NOTA using the method described below: Ac-Cys-$Z_{IGF\text{-}1R:4:40}$ was dissolved with freshly degassed phosphate buffer (0.1 M, pH 7.4) at a concentration of 1 mg/mL. MMA-NOTA (20 equivalents) dissolved in DMSO (10 mM) was added. After mixing by vortexing for 2 h, the desired product was purified by RP-HPLC with a protein-and-peptide C4 column (Grace Vydac 214TP54, Columbia, Maryland) using a gradient system of solvent A (0.1 % TFA/H2O) and solvent B (0.1 % TFA/acetonitrile). The flow rate was 4 mL/min, with the mobile phase starting from 90 % solvent A and 10 % solvent B (0–3 min) to 35 % solvent A and 65 % solvent B at 22 min. Fractions containing the product were collected and lyophilized. The identity of the products was confirmed using MALDI-TOF–MS.

Second, ^{64}Cu radiolabeling of NOTA-$Z_{IGF\text{-}1R:4:40}$ was performed. The Affibody conjugate NOTA-$Z_{IGF\text{-}1R:4:40}$ was radiolabeled with ^{64}Cu by the addition of 185 MBq $^{64}CuCl_2$ (1 μg of NOTA-$Z_{IGF\text{-}1R:4:40}$ per 3.7 MBq ^{64}Cu) in 0.1 N sodium acetate (NaOAc, pH 6.3) buffer followed by a 1-h incubation at 37 °C. EDTA (5 μL, 10 mM) was then added to quench the free ^{64}Cu. The radiolabeled complex was purified by a PD-10 column (GE Healthcare, Piscataway, NJ, USA). ^{64}Cu-NOTA-$Z_{IGF\text{-}1R:4:40}$ was reconstituted in PBS (0.1 M, pH 7.4) and passed through a 0.22-μm Millipore filter into a sterile vial for in vitro and animal experiments.

Cell assays

Cell uptake and receptor saturation assays were performed as previously described with minor modifications (Su et al. 2014). Briefly, the U87MG cell line was cultured in DMEM supplemented with 10 % FBS and 1 % penicillin–streptomycin. The cells were maintained in a humidified atmosphere of 5 % CO_2 at 37 °C, with the medium changed every 2 days. A 70–80 % confluent monolayer was detached by 0.1 % trypsin and dissociated into a single cell suspension for further cell culture.

Cell uptake assays

The U87MG cells were washed three times with PBS and dissociated with 0.25 % trypsin–EDTA. DMEM medium was then added to neutralize trypsin–EDTA. Cells were spun down and re-suspended with serum free DMEM. Cells (0.5×10^6) were incubated at 37 °C for 0.25–2 h with 7.4×10^{-3} MBq ^{64}Cu-NOTA-$Z_{IGF\text{-}1R:4:40}$ in 0.5 mL serum-free DMEM medium. The non-specific binding of the probes with U87MG cells was determined by co-incubation with 0.6 μM unlabeled NOTA-$Z_{IGF\text{-}1R:4:40}$. The cells were washed three times with 0.01 M PBS (pH 7.4) at room temperature. The cells were then washed three times with chilled PBS and spun down at a speed of 7000–8000 rpm. The cell pellets at the bottom of the tube were spliced, and the radioactivity of the pellets was measured using a γ-counter (PerkinElmer 1470, Waltham, MA). The uptake (counts/min) was normalized to the percentage of binding for analysis using Excel (Microsoft Software Inc., Redmond, Washington).

Receptor saturation assay

U87MG cells (0.3×10^6) were plated on 6-well plates 1 day before the experiment. Cells were washed with PBS three times. Serum-free DMEM (1 mL) was added to each well, followed by the addition of ^{64}Cu-NOTA-$Z_{IGF\text{-}1R:4:40}$ ($11.1–599.4 \times 10^{-3}$ MBq, 2–120 nM final concentration). The non-specific binding of ^{64}Cu-NOTA-$Z_{IGF\text{-}1R:4:40}$ with U87MG cells was determined by co-incubation with 100 times excess (0.6 μM) of NOTA-$Z_{IGF\text{-}1R:4:40}$. The plates were then put on ice for 2 h, and the cells were washed with cold PBS three times and detached with TrypLE-Express. The radioactivity of the cells was measured using a γ-counter. Specific binding (SB) = Total binding (TB) − non-specific binding (NSB). The data were analyzed using GraphPad Prism (GraphPad Software, Inc., San Diego, California), and the dissociation constant (K_D value) of ^{64}Cu-NOTA-$Z_{IGF\text{-}1R:4:40}$ was calculated from a 1-site-fit binding curve.

In vitro and in vivo stability

In vitro and in vivo stability were determined similarly to the procedures previously described with minor modifications (Miao et al. 2010; Su et al. 2014).

In vitro serum stability assay

^{64}Cu-NOTA-$Z_{IGF\text{-}1R:4:40}$ (4.44 MBq) in 250 μL of PBS was added to 2.0 mL of mouse serum and was incubated at 37 °C for 1, 4, and 24 h. At each time point, the mixture (0.74–1.85 MBq) was precipitated with 300 μL of ethanol and centrifuged at 16,000g for 2 min. The supernatant was transferred to a new Eppendrof tube, and DMF (300 μL) was added to precipitated the residue of serum protein. After centrifugation, the supernatant was acidified with 300 μL of buffer A (water + 0.1 % TFA) and filtered using a 0.2 μm nylon Spin-X column (Corning Inc. Corning, New York). The filtrates were then analyzed by radio-HPLC under conditions identical to the ones used to analyze the original radiolabeled compound. The percentage of intact of ^{64}Cu-NOTA-$Z_{IGF\text{-}1R:4:40}$ were determined by quantifying peaks corresponding to the intact and the degradation products.

In vivo stability assay

Two groups of U87MG mice (for each group $n = 3$) were injected with ^{64}Cu-NOTA-$Z_{IGF\text{-}1R:4:40}$ (7.4 MBq) via a tail vein and euthanized at 1 h after injection. The tumors and liver were removed and homogenized with DMF (0.5 mL) with 1 % Triton X-100 (Sigma-Aldrich, St.Louis, Missouri). Blood samples were centrifuged immediately after collection to remove the blood cells. The plasma portions or urine were added to DMF (0.5 mL) with 1 % Triton X-100. After centrifugation, the supernatant portions were diluted with solution A (99.9 % H_2O with 0.1 % TFA) and centrifuged again at 16,000g for 2 min with a nylon filter. The filtrates were analyzed by radio-HPLC under

conditions identical to those used for analyzing the original radiolabeled peptide.

Biodistribution studies

The animal procedures were performed according to a protocol approved by the Stanford University Institutional Animal Care and Use Committee. Approximately 5×10^6 cultured U87MG cells suspended in PBS were implanted subcutaneously in the right upper shoulders of nude mice. Tumors were allowed to grow to around 0.5–1.0 cm in diameter (25–30 days) and then the tumor-bearing mice were subject to in vivo biodistribution and imaging studies.

For biodistribution studies, U87MG tumor-bearing mice (for each group $n = 4$) were injected with ^{64}Cu-NOTA-$Z_{IGF\text{-}1R:4:40}$ (3.51–6.21 MBq) through the tail vein. At 24 h after injection, the mice were killed, tumors and normal tissues of interest were removed and weighed, and their radioactivity was measured in a γ-counter. The radioactivity uptake in the tumor and normal tissues was expressed as a percentage of the injected radioactivity per gram of tissue (%ID/g). In order to study the in vivo IGF-1R targeting specificity of ^{64}Cu-NOTA-$Z_{IGF\text{-}1R:4:40}$, unlabeled NOTA-$Z_{IGF\text{-}1R:4:40}$ protein (300 μg) was co-injected with ^{64}Cu-NOTA-$Z_{IGF\text{-}1R:4:40}$ in nude mice bearing A431 tumors ($n = 4$) via a tail vein, and biodistribution studies were conducted at 24 h after injection.

Small-animal PET imaging

PET imaging of tumor-bearing mice was performed on a microPET R4 rodent model scanner (Siemens Medical Solutions USA, Inc., Malvern, Pennsylvania). The mice bearing U87MG tumor (for each group $n = 4$) were injected with ^{64}Cu-NOTA-$Z_{IGF\text{-}1R:4:40}$ (3.51–6.21 MBq) with or without co-injection of unlabeled NOTA-$Z_{IGF\text{-}1R:4:40}$ protein through the tail vein. At 1, 2, 4, and 24 h after injection, the mice were anesthetized with 2 % isoflurane and placed near the center of the field of view of the microPET scanner in the prone position. Three-minute static scans were obtained, and the images were reconstructed by a two-dimensional ordered subsets expectation maximum (OSEM) algorithm. No background correction was performed. Regions of interest (ROIs; 5 pixels for coronal and transaxial slices) were drawn over the tumors on decay-corrected whole-body coronal images. The maximum counts per pixel per minute were obtained from the ROIs and converted to counts per milliliter per minute using a calibration constant. Tissue density was assumed to be 1 g/mL, and the ROIs were converted to counts per gram per minute. Image ROI-derived %ID/g values were determined by dividing counts per gram per minute by the injected dose. No attenuation correction was performed.

Statistical methods

Statistical analysis was performed using Student's two-tailed *t* test for unpaired data. A 95 % confidence level was chosen to determine the significance between groups, with a *P* values less than 0.05 being indicated as a significant difference.

Results

Chemistry and radiochemistry

The Affibody molecules Ac-Cys-$Z_{IGF\text{-}1R:4:40}$ with a cysteine at the C-terminal were successfully synthesized using conventional solid-phase peptide synthesis and purified by semi-preparative HPLC. The peptides were generally obtained in 10 % yield. The retention times on analytical HPLC were found to be 22 min. The purified Ac-Cys-$Z_{IGF\text{-}1R:4:40}$ was characterized by MALDI-TOF–MS. The measured molecular weight (MW) for its construct was consistent with the expected MWs (calculated MW = 6493.0 and found MW = 6493.36). Ac-Cys-$Z_{IGF\text{-}1R:4:40}$ was then conjugated with MMA-NOTA and purified by HPLC. The measured MW of the final product (NOTA-$Z_{IGF\text{-}1R:4:40}$) was $m/z = 6915.36$ for $[M + H]^+$ (calculated $MW^+_{[M+H]} = 6915.0$), and the purity for NOTA-$Z_{IGF\text{-}1R:4:40}$ was over 95 % (retention time 24 min).

The whole radiosynthesis of ^{64}Cu-NOTA-$Z_{IGF\text{-}1R:4:40}$ was accomplished within 60 min. Under HPLC conditions described above, ^{64}Cu-NOTA-$Z_{IGF\text{-}1R:4:40}$ showed a retention time of 24 min. The product was found to be more than 95 % radiochemically pure, as determined by analytic HPLC. The overall radiochemical yields with decay correction to the end of synthesis for ^{64}Cu-NOTA-$Z_{IGF\text{-}1R:4:40}$ were 75 %, with a specific activity of approximately 22.2×10^3 MBq/μmol.

Cell binding assays

Cell uptake levels for ^{64}Cu-NOTA-$Z_{IGF\text{-}1R:4:40}$ are shown in Fig. 2a. ^{64}Cu-NOTA-$Z_{IGF\text{-}1R:4:40}$ quickly accumulated in U87MG cells and reached a highest value of 7.82 % of applied activity at 1 h. When the probe was incubated with large excesses of unlabeled NOTA-$Z_{IGF\text{-}1R:4:40}$, its uptake levels in U87MG cells were significantly inhibited ($P < 0.05$) at all incubation time points.

The binding affinity of ^{64}Cu-NOTA-$Z_{IGF\text{-}1R:4:40}$ to IGF-1R was determined through the receptor saturation assay. As shown in Fig. 2b, the mean ± SD of K_D value of ^{64}Cu-NOTA-$Z_{IGF\text{-}1R:4:40}$ was 28.55 ± 3.95 nM. Overall, these results suggested that PET probe ^{64}Cu-NOTA-$Z_{IGF\text{-}1R:4:40}$ had high IGF-1R binding specificity and affinity, which warranted their further evaluation in vivo.

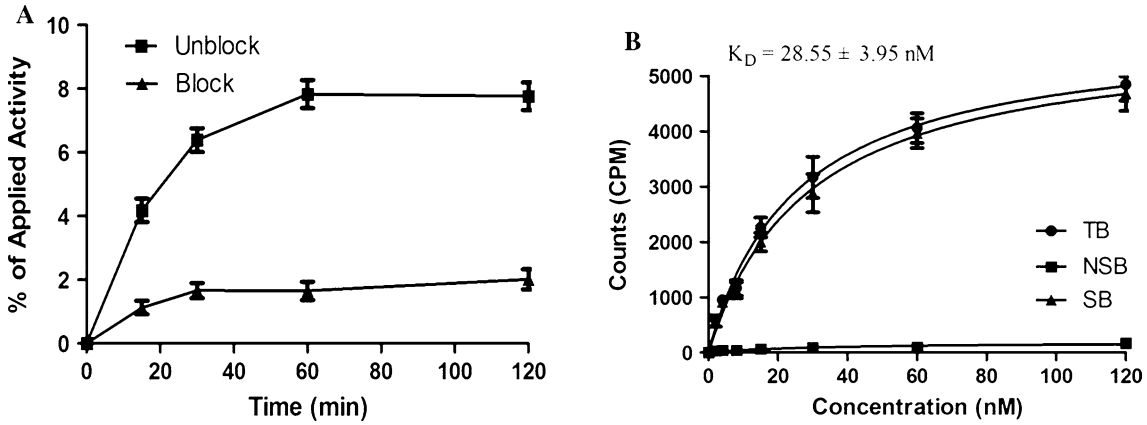

Fig. 2 Uptake (**a**) and binding affinity assay (**b**) of ^{64}Cu-NOTA-$Z_{IGF\text{-}1R:4:40}$ in U87MG cells

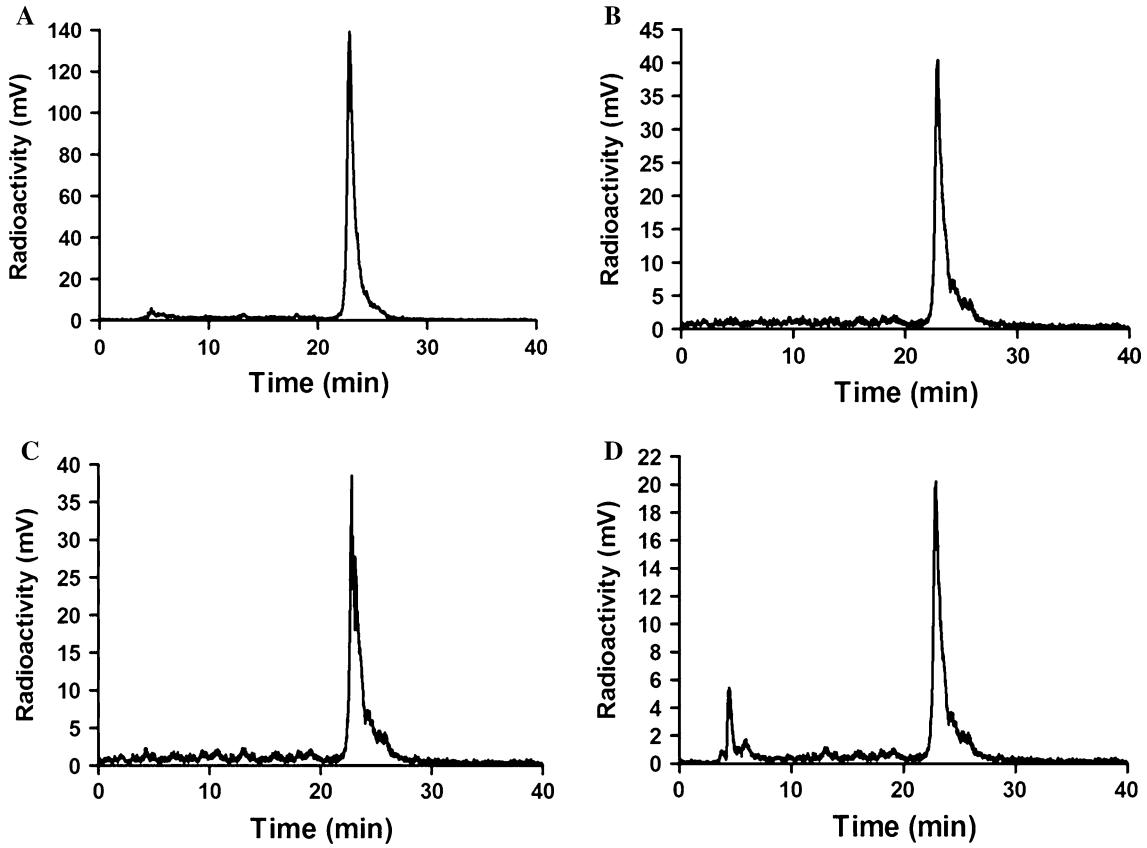

Fig. 3 HPLC radiochromatograms of purified ^{64}Cu-NOTA-$Z_{IGF\text{-}1R:4:40}$ (**a**) and radiolabeled probe after 1 h (**b**), 4 h (**c**), and 24 h (**d**) of incubation with mouse serum

In vitro stability and in vivo metabolite analysis

In vitro stability studies showed that more than 90 % of ^{64}Cu-NOTA-$Z_{IGF\text{-}1R:4:40}$ remained intact during 1–4 h of incubation in mouse serum, and there was about 75 % intact ^{64}Cu-NOTA-$Z_{IGF\text{-}1R:4:40}$ even after 24 h of incubation (Fig. 3b–d).

The in vivo stability studies are shown in Fig. 4a–d. At 1 h after injection, 90 %, and 85 % of ^{64}Cu-NOTA-$Z_{IGF\text{-}1R:4:40}$ remained intact in tumor, and plasma, respectively, while 55 % of the intact probe was observed in the urine, indicating relatively rapid degradation of the probe in the kidney–urinary systems. These studies demonstrate that the excellent in vivo stability of ^{64}Cu-NOTA-$Z_{IGF\text{-}1R:4:40}$, which

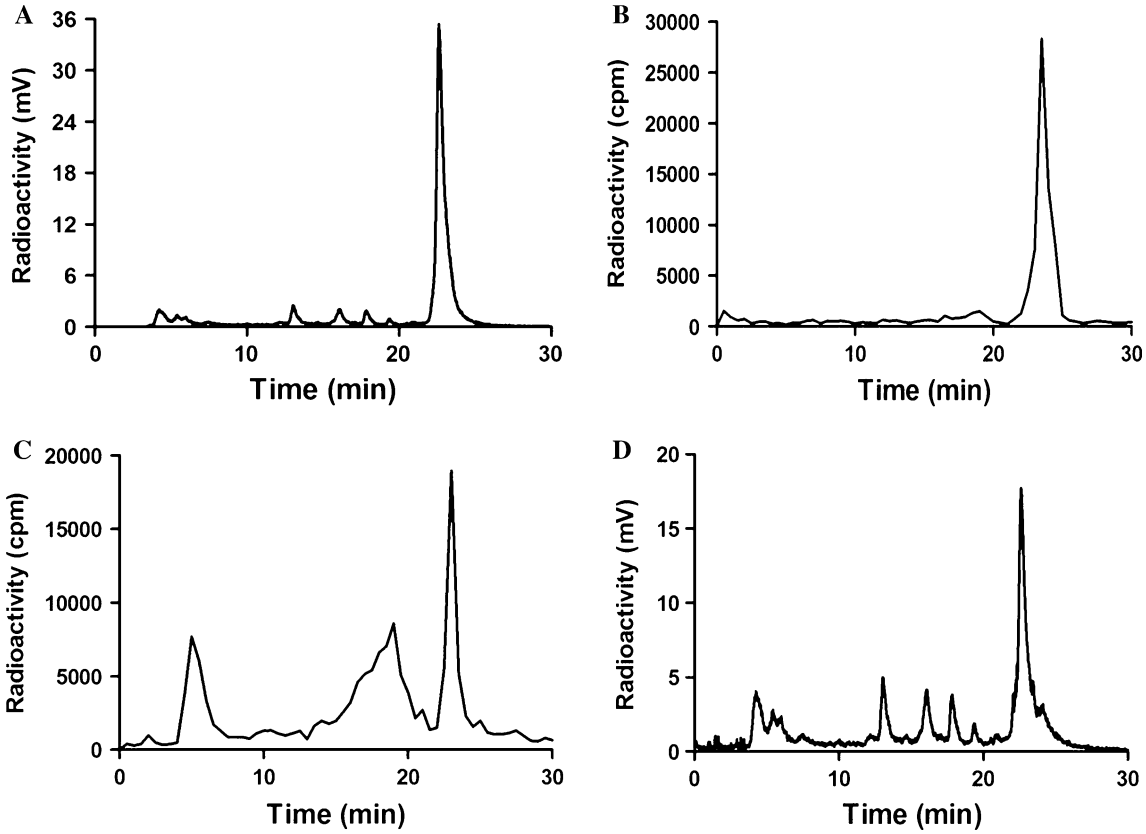

Fig. 4 In vivo metabolic stability assay of ^{64}Cu-NOTA-$Z_{IGF\text{-}1R:4:40}$ from samples of plasma (**a**), tumor (**b**), liver (**c**), and urine (**d**) at 1 h after injection

provides the solid foundation for quantitative imaging of IGF-1R expression in vivo using this PET probe. The HPLC result also showed that a small fraction of probe was metabolized in liver.

Biodistribution studies

At 24 h after injection, the biodistribution profiles of ^{64}Cu-NOTA-$Z_{IGF\text{-}1R:4:40}$ are presented in Table 1. ^{64}Cu-NOTA-$Z_{IGF\text{-}1R:4:40}$ displayed relatively high levels of radioactivity accumulation in U87MG tumors (5.08 ± 1.07 %ID/g), moderate levels in lung, pancreas, and stomach (3.57 ± 1.10, 2.97 ± 0.71, and 3.24 ± 1.50 %ID/g, respectively), and significantly high levels in the kidney and liver (63.02 ± 4.0, and 9.50 ± 1.13 %ID/g, respectively). Lower levels of radioactivity were observed in muscle, brain, bone, and blood (0.44 ± 0.15, 0.30 ± 0.09, 1.00 ± 0.21, and 1.27 ± 0.37 %ID/g, respectively).

For the in vivo blocking study, ^{64}Cu-NOTA-$Z_{IGF\text{-}1R:4:40}$ was co-injected with a large excess (300 μg) of the unlabeled NOTA-$Z_{IGF\text{-}1R:4:40}$ to saturate endogenous and overexpressed IGF-1R. The co-injection of NOTA-$Z_{IGF\text{-}1R:4:40}$ specifically reduced the tumor, lung, stomach, and pancreas uptake of ^{64}Cu-NOTA-$Z_{IGF\text{-}1R:4:40}$ at 24 h after injection ($P < 0.05$), whereas the liver, kidney, blood, spleen, muscle, and bone uptake are not significantly changed in the blocking group ($P > 0.05$). ^{64}Cu-NOTA-$Z_{IGF\text{-}1R:4:40}$ provided significantly high tumor-to-muscle ratios and lower tumor-to-liver and tumor to kidney ratios (Table 1).

Small-animal PET imaging

Small animal PET images acquired at 1, 2, 4, and 24 h after injection of ^{64}Cu-NOTA-$Z_{IGF\text{-}1R:4:40}$ are shown in Fig. 5. The U87MG tumor was clearly visualized, with good tumor-to-background contrast, at 1–24 h after injection. Also observed were high levels of radioactivity accumulation in the kidneys and liver.

The activity accumulation of ^{64}Cu-NOTA-$Z_{IGF\text{-}1R:4:40}$ in the U87MG tumor and other organs was also quantified (Fig. 6). Time–activity curves for the tumor and the contralateral muscle tissue are shown in Fig. 7. These results showed higher tumor uptake, moderate uptake in the lungs, and low uptake in the muscles. The uptake values (%ID/g) of tumor and the other organs obtained from PET image data at 24 h after injection were consistent

Table 1 Biodistribution results for ^{64}Cu-NOTA-$Z_{IGF\text{-}1R:4:40}$ in U87MG xenogratfs

Organ (%ID/g) (spiked dose)	^{64}Cu-NOTA-$Z_{IGF\text{-}1R:4:40}$ (24 h)	
	0 μg dose, unblock	300 μg dose, block
Blood	1.27 ± 0.37	0.96 ± 0.21
Heart	2.46 ± 0.70	2.09 ± 0.29
Lung	3.57 ± 1.10[a]	1.42 ± 0.45[a]
Liver	9.50 ± 1.13	8.07 ± 0.77
Spleen	2.20 ± 0.52	1.64 ± 0.23
Pancreas	2.97 ± 0.71[a]	1.10 ± 0.14[a]
Stomach	3.24 ± 1.50[a]	1.16 ± 0.33[a]
Brain	0.30 ± 0.09	0.24 ± 0.06
Intestine	1.73 ± 0.54	1.34 ± 0.44
Kidneys	63.02 ± 4.00	59.26 ± 5.58
Skin	1.49 ± 0.51	1.58 ± 0.25
Muscle	0.44 ± 0.15	0.32 ± 0.04
Bone	1.00 ± 0.21	0.77 ± 0.12
Tumor	5.08 ± 1.07[a]	1.48 ± 0.86[a]
Uptake ratio		
Tumor to blood	4.09 ± 0.59[b]	1.61 ± 0.93[b]
Tumor to lung	1.46 ± 0.18	1.18 ± 0.98
Tumor to muscle	11.89 ± 2.16[b]	4.66 ± 2.75[b]
Tumor to liver	0.53 ± 0.06[b]	0.19 ± 0.14[b]
Tumor to kidney	0.08 ± 0.02[b]	0.02 ± 0.01[b]
Tumor to bone	5.10 ± 0.49[b]	2.07 ± 1.62[b]

Data are mean ± SD, expressed as %ID/g. Student's unpaired two-tailed *t* test was conducted

[a, b] $P < 0.05$, comparing 0 μg (unblock) and 300 μg (block) of dose tracer biodistribution at 24 h after injection with ^{64}Cu-NOTA-$Z_{IGF\text{-}1R:4:40}$

with the findings obtained in the biodistribution studies. Moreover, when co-injected with 300 μg (block dose) of unlabeled NOTA-$Z_{IGF\text{-}1R:4:40}$, the tumor was barely visible on PET images at 1–24 h after injection (Fig. 5). A quantitative analysis of PET images showed significantly lower tumor uptake for mice injected with 300 μg blocking dose compared to that in without co-injection of unlabeled NOTA-$Z_{IGF\text{-}1R:4:40}$ ($P < 0.05$) at all time points (1–24 h post-injection). The PET scans also revealed that most ^{64}Cu-NOTA-$Z_{IGF\text{-}1R:4:40}$ was quickly cleared through the renal–urine system.

Discussion

The insulin-like growth factor 1 receptor (IGF-1R) plays an essential role in the development, progression, and invasion of various types of cancers. Inhibition of IGF-1R signaling thus appears to be a promising approach for cancer therapy. Several IGF-1R targeting strategies, such as monoclonal antibodies and tyrosine kinase inhibitors, are being investigated in phases I and II clinical trials (Pollak 2012; Haisa 2013). Patients with cancer lesions that express IGF-1R may benefit from IGF-1R targeted therapy. Clinical trials have shown that there is an urgent unmet clinical need for the development of predictive biomarkers permitting patient selection for such therapy (Zha et al. 2009; Gong et al. 2009; Ozkan 2011). The IGF-1R targeted SPECT molecular probes have been demonstrated to provide a real-time assay of IGF-1R expression in living subjects (Tolmachev et al. 2012; Orlova et al. 2013; Mitran et al. 2015). Furthermore, PET imaging is particularly useful because of its high sensitivity, high spatial resolution, strong quantification ability, and its great potential for clinical translation. Combining the aforementioned optimal clinical characteristics to develop an imaging agent is significantly important since our goal is to ultimately apply Affibody-based PET probes for imaging patients.

Affibody molecules have been demonstrated good in vivo stability and bioavailability (Miao et al. 2010; Su et al. 2014). In this study, an Affibody molecule analogue Ac-Cys-$Z_{IGF\text{-}1R:4:40}$ was site-specifically conjugated with a versatile chelator MMA-NOTA, labeled with ^{64}Cu, and then measured the binding specificity and affinity to IGF-1R. The probe ^{64}Cu-NOTA-$Z_{IGF\text{-}1R:4:40}$ showed good binding affinity to the U87MG cell IGF-1R with a K_D of 28.55 ± 3.95 nM (Fig. 2a), which is similar to that of ^{64}Cu-DOTA-$Z_{EGFR:1907}$ (20 nM) (Miao et al. 2010), but was lower than that of unmodified Affibody molecule $Z_{IGF\text{-}1R:4:40}$ (~2.3 nM) (Li et al. 2010), $[^{99m}Tc(CO)_3]^+$-$(HE)_3$-$Z_{IGF1R:4551}$ (1.7 ± 0.5 nM) (Orlova et al. 2013) and ^{99m}Tc-$Z_{IGF1R:4551\text{-}GGGC}$ (12 nM) (Mitran et al. 2015). Such difference may be taken for three reasons. First, IGR-1R receptor presents two binding sites, one with higher affinity (844 pM) and one with lower affinity (12 nM) (Mitran et al. 2015). $Z_{IGF1R:4551}$ binds to two binding sites on IGF-1R (Orlova et al. 2013). Second, the Affibody molecule Ac-Cys-$Z_{IGF\text{-}1R:4:40}$ maybe tolerating some C-terminal modifications. Third, the models were different, which can be associated with different levels of IGF-1R expression. In vitro cell uptake experiments showed that ^{64}Cu-NOTA-$Z_{IGF\text{-}1R:4:40}$ had rapid accumulation in the U87MG cells. The uptake reached a plateau in 1 h. This accumulation is IGF-1R specific receptor binding since the rapid cellular uptake of the tracer could be effectively blocked by cold NOTA-$Z_{IGF\text{-}1R:4:40}$ (Fig. 2a), suggesting that labeling has not influenced the ability of $Z_{IGF\text{-}1R:4:40}$ to bind specifically to IGF-1R. These results warranted the further evaluation of the probe for in vivo IGF-1R-targeted tumor imaging.

Site-specifically labeled ^{64}Cu-NOTA-$Z_{IGF\text{-}1R:4:40}$ showed good in vivo pharmacokinetics for IGF-1R targeted PET imaging. ^{64}Cu-NOTA-$Z_{IGF\text{-}1R:4:40}$ exhibited rapid tumor accumulation and blood clearance, which are the major advantages of using these relatively small Affibody

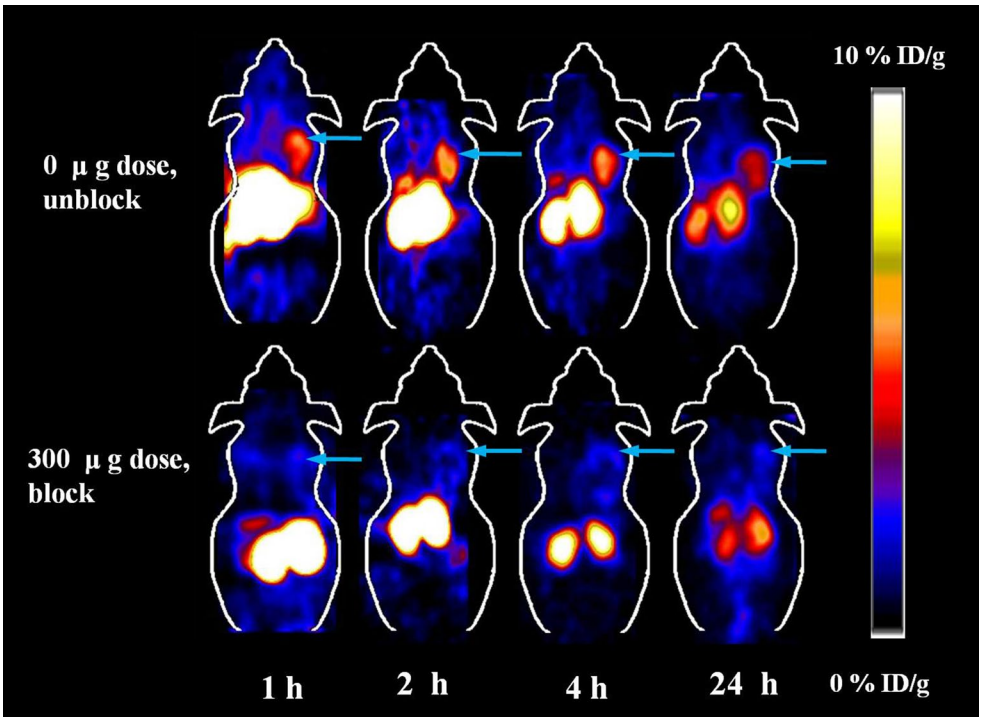

Fig. 5 Small-animal PET of ^{64}Cu-NOTA-$Z_{IGF\text{-}1R:4:40}$ in U87MG xenograft models co-injected with 0 µg dose (*unblock*) or 300 µg dose (*block*) of NOTA-$Z_{IGF\text{-}1R:4:40}$ at 1, 2, 4, and 24 h after injection (for each group $n = 4$)

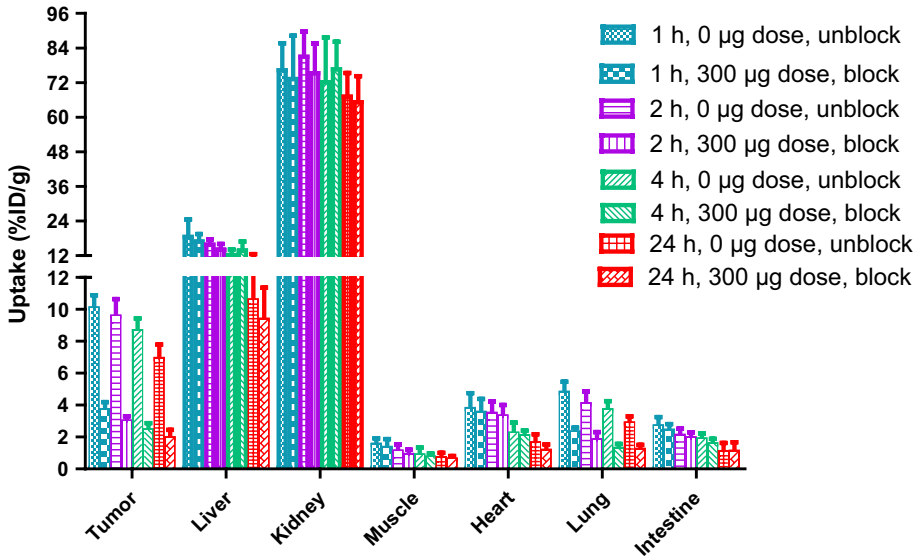

Fig. 6 PET quantification analysis for uptakes of tumor, liver, kidney, muscle, heart, lung, and intestine for ^{64}Cu-NOTA-$Z_{IGF\text{-}1R:4:40}$ in U87MG xenograft models co-injected with 0 µg dose (*unblock*) or 300 µg dose (*block*) of NOTA-$Z_{IGF\text{-}1R:4:40}$ at 1, 2, 4, and 24 h after injection (for each group $n = 4$)

molecules as imaging agents compared to large, long-circulating proteins such as full antibodies (Cheng et al. 2010). It rapidly localized in U87MG tumors and showed good tumor uptake, retention, and tumor-to-muscle ratios (Figs. 5, 6, 7). U87MG tumors could be clearly visualized by PET at 1–24 h after injection, with good contrast. It is also interesting to find out that the tumor uptake of the ^{64}Cu-NOTA-$Z_{IGF\text{-}1R:4:40}$, and tumor to muscle ratio are higher than those of the ^{111}In-DOTA-$Z_{IGFIR:4551}$ (Tolmachev et al. 2012), [^{99m}Tc(CO)$_3$]$^+$-(HE)$_3$-$Z_{IGF1R:4551}$ (Orlova et al. 2013) and ^{99m}Tc-$Z_{IGF1R:4551}$-GGGC (Mitran et al. 2015), while the kidney uptake of the probe, and tumor-to-blood ratio are much lower compared to ^{111}In-DOTA-$Z_{IGFIR:4551}$ (Tolmachev et al. 2012). Evaluation of the probe in mice demonstrated that ^{64}Cu-NOTA-$Z_{IGF\text{-}1R:4:40}$ is a promising agent for IGF-1R imaging.

In this study, the kidney and liver showed the highest uptake because they are the major organs of metabolism. In agree with previous study (Tolmachev et al. 2012; Orlova et al. 2013; Mitran et al. 2015), radioactivity was found in the lung, pancreas, and stomach since these normal organs have moderate IGF-1R expression. A high expression of

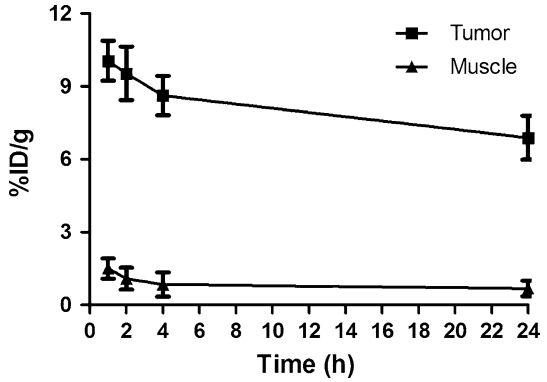

Fig. 7 Tumor and muscle time–activity curves derived from multiple-time-point small-animal PET images in U87MG xenograft models at 1, 2, 4, and 24 h after the injection of ^{64}Cu-NOTA-$Z_{IGF\text{-}1R:4:40}$. Data are shown as mean ± SD (%ID/g) ($n = 4$)

the target in normal organ might appreciably influence the imaging results, especially when the target level in the tumor is low. After optimization of spiking doses was administered to saturate the target expression in normal organ, an increased tumor-normal ratio could be achieved (Tolmachev et al. 2012; Su et al. 2014). The in vivo IGF-1R binding specificity of ^{64}Cu-NOTA-$Z_{IGF\text{-}1R:4:40}$ was also verified. Uptakes of the probe in high IGF-1R expression tissues including tumor, lung, pancreas and stomach were all significantly reduced at 24 h after injection of the block agent (300 μg of Ac-Cys-$Z_{IGF\text{-}1R:4;40}$ ($P < 0.05$). High kidney accumulation may interfere with the visualization of tumor lesions located in the kidney. There are indications for which IGF-1R imaging with ^{64}Cu-NOTA-$Z_{IGF\text{-}1R:4:40}$ could be improved by developing approaches to minimize the reabsorption of Affibody molecules by the kidneys. These potential approaches of reducing kidney uptake include the use of positively charged amino acids, gelofusin or album fragments (Rolleman et al. 2003; van Eerd et al. 2006; Vegt et al. 2008).

Imaging of IGF-1R expression in vivo is not only valuable for treatment optimization of cancer patients, but also may be useful for identifying HER2-positive tumors in the patients with breast cancer that are resistant to trastuzumab through this mechanism, because there was a direct relationship between IGF-1R density and the resistance of these cells to trastuzumab in vitro (Cornelissen et al. 2008). Furthermore, IGF-1R signaling has been suggested to be involved in development of gefitinib resistance in non-small cell lung cancer (Morgillo et al. 2007). Thus, further research for imaging of IGF-1R expression has high clinical translational ability and will likely find broad applications in patient therapy and management for targeting the expression of IGF-1R and cross-talk between HER2 and IGF-1R signaling.

In conclusion, an anti-IGF-1R Affibody molecule Ac-Cys-$Z_{IGF\text{-}1R:4:40}$ has been successfully radiolabeled with ^{64}Cu. ^{64}Cu–NOTA-$Z_{IGF\text{-}1R:4:40}$ shows favorable in vivo profiles and excellent tumor imaging quality, and it is a promising PET probe for imaging IGF-1R positive tumor.

Acknowledgments This work was supported in part by the Office of Science (BER), US Department of Energy (DE-SC0008397), National Natural Science Foundation of China (81071182) and Medical Innovation Foundation of Fujian, China (2009-CXB-46).

Conflict of interest The authors declare that they have no conflict of interest.

Ethical approval The animal procedures were performed according to a protocol approved by the Stanford University Institutional Animal Care and Use Committee. This article does not contain any studies with human participants performed by any of the authors.

Informed consent Not available since no human study was involved.

References

Ait-Mohand S, Fournier P, Dumulon-Perreault V, Keifer GE, Jurek P, Ferreira CL, Bénard F, Guérin B (2011) Evaluation of ^{64}Cu-labeled bifunctional chelate-bombesin conjugates. Bioconjug Chem 22:1729–1735

Arcaro A (2013) Targeting the insulin-like growth factor-1 receptor in human cancer. Front Pharmacol 4:30

Cheng Z, De Jesus OP, Kramer DJ, De A, Webster JM, Gheysens O, Levi J, Namavari M, Wang S, Park JM, Zhang R, Liu H, Lee B, Syud FA, Gambhir SS (2010) ^{64}Cu-labeled Affibody molecules for imaging of HER2 expressing tumors. Mol Imaging Biol 12:316–324

Cornelissen B, McLarty K, Kersemans V, Reilly RM (2008) The level of insulin growth factor-1 receptor expression is directly correlated with the tumor uptake of ^{111}In-IGF-1(E3R) in vivo and the clonogenic survival of breast cancer cells exposed in vitro to trastuzumab (Herceptin). Nucl Med Biol 35:645–653

Fleuren ED, Versleijen-Jonkers YM, van de Luijtgaarden AC, Molkenboer-Kuenen JD, Heskamp S, Roeffen MH, van Laarhoven HW, Houghton PJ, Oyen WJ, Boerman OC, van der Graaf WT (2011) Predicting IGF-1R therapy response in bone sarcomas: immuno-SPECT imaging with radiolabeled R1507. Clin Cancer Res 17:7693–7703

Friedman M, Nordberg E, Höidén-Guthenberg I, Brismar H, Adams GP, Nilsson FY, Carlsson J, Stahl S (2007) Phage display selection of affibody molecules with specific binding to the extracellular domain of the epidermal growth factor receptor. Protein Eng Des Sel 20:189–199

Gong Y, Yao E, Shen R, Goel A, Arcila M, Teruya-Feldstein J, Zakowski MF, Frankel S, Peifer M, Thomas RK, Ladayi M, Pao W (2009) High expression levels of total IGF-1R and sensitivity of NSCLC cells in vitro to an anti-IGF-1R antibody (R1507). PLoS One 4:e7273

Haisa M (2013) The type 1 insulin-like growth factor receptor signalling system and targeted tyrosine kinase inhibition in cancer. J Int Med Res 41:253–264

Heskamp S, van Laarhoven HW, Molkenboer-Kuenen JD, Bouwman WH, van der Graaf WT, Oyen WJ, Boerman OC (2012) Optimization of IGF-1R SPECT/CT imaging using ^{111}in-labeled F(ab')

(2) and fab fragments of the monoclonal antibody R1507. Mol Pharm 9:2314–2321

Li J, Lundberg E, Vernet E, Larsson B, Höidén-Guthenberg I, Gräslund T (2010) Select-ion of affibody molecules to the ligand-binding site of the insulin-like growth factor-1 receptor. Biotechnol Appl Biochem 55:99–109

Miao Z, Ren G, Liu H, Jiang L, Cheng Z (2010) Small-animal PET imaging of human epidermal growth factor receptor positive tumor with a ^{64}Cu labeled Affibody protein. Bioconjug Chem 21:947–954

Miao Z, Ren G, Liu H, Qi S, Wu S, Cheng Z (2012) PET of EGFR expression with an ^{18}F-labeled Affibody molecule. J Nucl Med 53:1110–1118

Mitran B, Altai M, Hofström C, Honarvar H, Sandström M, Orlova A, Tolmachev V, Gräslund T (2015) Evaluation of ^{99m}Tc-ZIGF1R:4551-GGGC Affibody molecule, a new probe for imaging of insulin-like growth factor type 1 receptor expression. Amino Acids 47:303–315

Morgillo F, Kim WY, Kim ES, Ciardiello F, Hong WK, Lee HY (2007) Implication of the insulin-like growth factor-IR pathway in the resistance of non-small cell lung cancer cells to treatment with gefitinib. Clin Cancer Res 13:2795–2803

Orlova A, Hofström C, Strand J, Varasteh Z, Sandstrom M, Andersson K, Tolmachev V, Gräslund T (2013) [99mTc(CO)3]+-(HE)3-ZIGF1R:4551, a new Affibody conjugate for visualization of insulin-like growth factor-1 receptor expression in malignant tumours. Eur J Nucl Med Mol Imaging 40:439–449

Ozkan EE (2011) Plasma and tissue insulin-like growth factor-I receptor (IGF-IR) as a prognostic marker for prostate cancer andanti-IGF-IR agents as novel therapeutic strategy for refractory cases: a review. Mol Cell Endocrinol 344:1–24

Pollak M (2008) Insulin and insulin-like growth factor signaling in neoplasia. Nat Rev Cancer 8:915–927

Pollak M (2012) The insulin receptor/insulin-like growth factor receptor family as a therapeutic target in oncology. Clin Cancer Res 18:40–50

Prasanphanich AF, Nanda PK, Rold TL, Ma L, Lewis MR, Garrison JC, Hoffman TJ, Sieckman GL, Figueroa SD, Smith CJ (2007) [^{64}Cu-NOTA-8-Aoc-BBN (7-14)NH2] targeting vector for positron-emission tomography imaging of gastrinreleasing peptide receptor-expressing tissues. Proc Natl Acad Sci USA 104:12462–12467

Ren G, Webster JM, Liu Z, Zhang R, Miao Z, Liu H, Gambhir SS, Syud FA, Cheng Z (2012) In vivo targeting of HER2-positive tumor using 2-helix affibody molecules. Amino Acids 43:405–413

Rolleman EJ, de Valkema JM R, Kooij PP, Krenning EP (2003) Safe and effective inhibition of renal uptake of radiolabelled octreotide by a combination of lysine and arginine. Eur J Nucl Med Mol Imaging 30:9–15

Singh P, Alex JM, Bast F (2014) Insulin receptor (IR) and insulin-like growth factor receptor 1 (IGF-1R) signaling systems: novel treatment strategies for cancer. Med Oncol 31:805

Su X, Cheng K, Jeon J, Shen B, Venturin GT, Hu X, Rao J, Chin FT, Wu H, Cheng Z (2014) Comparison of two site-specifically ^{18}F-labeled Affibodies for PET imaging of EGFR positive tumors. Mol Pharm 11:3947–3956

Tolmachev V, Stone-Elander S, Orlova A (2010) Current approaches to the use of radiolabeled tyrosine kinase-targeting drugs for patient stratification and treatment response monitoring: prospects and pitfalls. Lancet Oncol 11:992–1000

Tolmachev V, Malmberg J, Hofström C, Abrahmsén L, Bergman T, Sjöberg A, Sandström M, Gräslund T, Orlova A (2012) Imaging of insulinlike growth fact-or type 1 receptor in prostate cancer xenog-rafts using the Affibody molecule ^{111}In-DOTA-ZIGF1R:4551. J Nucl Med 53:90–97

van Eerd JE, Vegt E, Wetzels JF, Russel FG, Masereeuw R, Corstens FH, Oyen WJ, Boerman OC (2006) Gelatin-based plasma expander effectively reduces renal uptake of 111In-octreotide in mice and rats. J Nucl Med 47:528–533

Vegt E, van Eerd JE, Eek A, Oyen WJ, Wetzels JF, de Jong M, Russel FG, Masereeuw R, Gotthardt M, Boerman OC (2008) Reducing renal uptake of radiolabeled peptides using albumin fragments. J Nucl Med 49:1506–1511

Xue M, Cao X, Zhong Y, Kuang D, Liu X, Zhao Z, Li H (2012) Insulin-like growth factor-1 receptor (IGF-1R) kinase inhibitors in cancer therapy: advances and perspectives. Curr Pharm Des 18:2901–2913

Zha J, O'Brien C, Savage H, Huw LY, Zhong F, Berry L, Lewis Philips GD, Luis E, Cavet G, X H, Amler LC, Lackner MR (2009) Molecular predictors of response to a humanized anti-insulin-like growth factor-I receptor monoclonal antibody in breast and colorectal cancer. Mol Cancer Ther 8:2110–21121

Zhang Y, Hong H, Engle JW, Bean J, Yang Y, Leigh BR, Barnhart TE, Cai W (2011) Positron emission tomography imaging of CD105 expression with a ^{64}Cu-labeled monoclonal anti-body: NOTA is superior to DOTA. PLoS One 6:e28005